Heliyon 9 (2023) e16083

Contents lists available at ScienceDirect

Heliyon

journal homepage: www.cell.com/heliyon

Research article

Metabolomics and network analysis uncovered profound inflammation-associated alterations in hepatitis B virus-related cirrhosis patients with early hepatocellular carcinoma

Zhiyong Du [a,1], Shengju Yin [b,e,f,1], Bing Liu [b], Wenxin Zhang [b], Jiaxu Sun [b], Meng Fang [b], Yisheng Xu [g], Kun Hua [a], Pengfei Tu [b], Guoliang Zhang [d,**], Ying Ma [c,***], Yingyuan Lu [b,*]

[a] *Beijing Anzhen Hospital, Capital Medical University, Beijing Institute of Heart Lung and Blood Vessel Disease, Beijing, 100029, China*
[b] *State Key Laboratory of Natural and Biomimetic Drugs, School of Pharmaceutical Sciences, Peking University, Beijing, 100191, China*
[c] *State Key Laboratory Breeding Base of Dao-di Herbs, National Resource Center for Chinese Materia Medica, China Academy of Chinese Medical Sciences, Beijing, 100700, China*
[d] *School of Basic Medical Sciences, Peking University, Beijing, 100191, China*
[e] *Shanghai Key Laboratory of Children's Environment Health, School of Public Health/Xinhua Hospital, Shanghai Jiao Tong University School of Medicine, Shanghai, 200025, China*
[f] *Shandong Jiaotong Hospital, Jinan, 250031, China*
[g] *Waters Technologies Ltd., Beijing, 102600, China*

ARTICLE INFO

Keywords:
Hepatocellular carcinoma
Liver cirrhosis
Hepatitis B virus
Metabolomics

ABSTRACT

Patients with hepatitis B virus (HBV)-related liver cirrhosis (LC) are at high risk for hepatocellular carcinoma (HCC). Limitations in the early detection of HCC give rise to poor survival in this high-risk population. Here, we performed comprehensive metabolomics on health individuals and HBV-related LC patients with and without early HCC. Compared to non-HCC patients (N = 108) and health controls (N = 80), we found that patients with early HCC (N = 224) exhibited a specific plasma metabolome map dominated by lipid alterations, including lysophosphatidylcholines, lysophosphatidic acids and bile acids. Pathway and function network analyses indicated that these metabolite alterations were closely associated with inflammation responses. Using multivariate regression and machine learning approaches, we identified a five-metabolite combination that showed significant performances in differentiating early-HCC from non-HCC than α-fetoprotein (area under the curve values, 0.981 versus 0.613). At metabolomic levels, this work provides additional insights of metabolic dysfunction related to HCC progressions and demonstrates the plasma metabolites might be measured to identify early HCC in patients with HBV-related LC.

* Corresponding author.
** Corresponding author.
*** Corresponding author.
E-mail addresses: GL168@bjmu.edu.cn (G. Zhang), xiaoma1110@126.com (Y. Ma), luyingyuan518@bjmu.edu.cn (Y. Lu).
[1] These authors contributed equally to this work.

https://doi.org/10.1016/j.heliyon.2023.e16083
Received 4 December 2022; Received in revised form 29 April 2023; Accepted 4 May 2023
Available online 9 May 2023

1. Introduction

Hepatocellular carcinoma (HCC) is the third leading cause of cancer-related deaths and the most common cause of death in patients with liver cirrhosis (LC) [1,2]. Infection by hepatitis B virus (HBV) is the main risk factor for HCC and LC [3,4]. Worldwide, HBV accounts for approximately one-third of LC cases and one-half of HCC [5]. In China, 77% of LC cases and 84% of HCC cases are caused by HBV infection [6]. It is well known that LC alone is also a strong risk factor leading to HCC. LC is found in more than 90% of patients with HCC [2]. However, the underlying mechanisms of the progression from HBV-related LC to HCC remain largely unknown.

The treatment of HCC remains challenging and is largely determined by early diagnosis. The overall 5-year survival for patients with HCC is very poor at 5% [7]. Early detection of preclinical or early symptomatic HCC offers the potential for improving survival [8]. For screening early HCC in a high-risk population of HBV-related LC patients, thorough surveillance by liver ultrasound is recommended. However, an important limitation of ultrasound is its low sensitivity for the differentiation of malignant from benign nodules in LC and its strong dependence on operator experience [9,10]. Serum α-fetoprotein (AFP), is the most widely used non-invasive marker of HCC in clinical practice. However, previous evidences indicated that AFP could not effectively differentiate early HCC from LC, because both LC and HCC could cause AFP elevation [11,12]. At present, the gold standard for diagnosing HCC is biopsy, which is not indicated in most HCC cases due to irreversible damage and concomitant risks [13]. Therefore, the identification of accurate and noninvasive biomarkers for screening and diagnosing early HCC in high-risk LC population is urgently needed.

Metabolic reprogramming is an important hallmark of cancer. Cancer cells undergo metabolic reprogramming to maintain tumorigenesis and cell proliferation [14,15]. Metabolomics, aiming to comprehensively study the entire metabolome in biological sample, is a newly emerged analytic discipline with promising potential in the area of precise medicines [16]. The progressive development of high-throughput metabolomic technologies makes it possible to provide comprehensive molecular data for understanding the biochemical perturbations in a variety of cancers, allowing for the discovery of potential therapeutic targets and diagnostic biomarkers [17,18]. Metabolomic studies from biofluids or tissues have indicated that HCC could present a variety of characteristic metabolic changes, such as imbalance of oxidative metabolism, dysregulation of amino acid, and phospholipid metabolism [19,20].

Despite several small-sample-size metabolomic studies have been performed to explore discriminatory profiles of HCC differentiated from HBV infection or LC [21–24], the deep metabolic profiling of early HCC in patients with HBV-related LC has not been systematically studied. Here, we used comprehensive metabolomics and network analysis to investigate the metabolic signatures in plasma samples from a large panel of HBV-related LC patients with and without early HCC (N = 332) and health controls (N = 80). Furthermore, we performed multivariable regression and machine learning analyses to identify candidate metabolite biomarkers for the early detection of HCC cases in patients with HBV-related LC.

2. Materials and methods

2.1. Study subjects

A total of 332 patients with HBV infection, including 224 LC patients with early-stage HCC and 108 LC patients without HCC were enrolled from Shandong Jiaotong Hospital and Anzhen Hospital between 2015 and 2021. In addition, age- and sex-matched healthy individuals (n = 80) were included. This study protocol was conducted in accordance with the Declaration of Helsinki and approved by the Ethics Committees of Peking university health sciences center. All participants provided written informed consent, which was the review procedure of the ethics committee.

The inclusion criteria were as follows: participants aged >18 years with HBV infection and defined LC. The diagnosis of LC and HCC was performed by two or more hepatogastroenterologists. LC diagnosis was based on the established basis of clinical LC symptoms, abnormal liver function, histology (progressive fibrosis, loss of hepatic architecture), and liver imaging (including abdominal ultrasonography, computed tomography, magnetic resonance imaging, or portal hypertension assessed by hepatic arteriography), when needed. In addition, patients with LC underwent liver imaging studies to exclude HCC within 6 months of registration. LC stage was assessed by Child-Pugh class. HCC cases were diagnosed based on well-established diagnostic liver imaging criteria and/or biopsy histology according to the criteria of Barcelona Clinic Liver Cancer (BCLC) and American Association for Study of Liver Disease Group [24]. Early HCC is defined as a single node of HCC measuring <3 cm, or up to 3 nodes <3 cm each, Child-Pugh A-B class [25]. Exclusion criteria for the study were current or historical conditions of other types of liver diseases for patients with nonalcoholic/alcoholic fatty liver diseases, autoimmune hepatitis, primary biliary cholangitis, and primary sclerosing cholangitis, current or no more than three months of acute cardiovascular and cerebrovascular diseases, respiratory diseases, ulcerative colitis, other infectious diseases (HIV, hepatitis C virus, hepatitis D), pregnancy, and definite HCC with anti-cancer therapy. HBV infection was defined as positive HBV surface antigen (HBsAg), hepatitis B virus DNA levels ≥20 IU/mL, and elevated aspartate aminotransferase (AST) or alanine aminotransferase (ALT) levels.

2.2. Clinical data collection

Demographic characteristics, including age, gender, body mass index, smoking and drinking status, were recorded for each study participant. Hypertension was defined as a condition in individuals with mean office systolic blood pressure (SBP) ≥ 140 mmHg or diastolic blood pressure (DBP) ≥ 90 mmHg or a defined history of hypertension. Diabetes mellitus was defined as a condition in individuals with clinical diagnosed type 1 and type 2 diabetes based on the American Diabetes Association. Patients who exhibited ≥50%

stenosis in at least one main coronary artery were diagnosed with coronary heart disease. Fasting blood samples were obtained to measure glucose, total cholesterol (TC), triglycerides (TG), low-density lipoprotein cholesterol (LDL-C), high-density lipoprotein cholesterol (HDL-C), total bilirubin (TBIL), direct bilirubin (DBIL), ALT, AST, and AFP using an automatic biochemistry analyzer (Beckman AU 5400, Brea, USA).

2.3. Metabolomic analysis

Sample preparation and ultra performance liquid chromatography system coupled with quadrupole-time of flight mass spectrometer (UPLC-Q-TOF/MS) based-metabolomics were performed according to previous protocols [26–28]. Briefly, the frozen plasma samples were thawed at 4 °C. A total of 200 μL of ice-cold methanol-water (7:3, v/v) containing 2 μg/mL lysophosphatidylcholine (LysoPC) 19:0-d_5, 3.5 μg/mL phosphatidylcholine (PC) 18:0/20:4-d_{11}, 1.52 μg/mL tauroursodeoxycholic acid-d_4, 2 μg/mL glycocholic acid-d_4, 4.3 2 μg/mL stearoyl-L-carnitine-d_3, 1.5 μg/mL L-arginine-d_7, 2.4 μg/mL L-phenyl-d_5-alanine, 1.2 μg/mL L-leucine-5, 5,5-d_3, and 3.2 μg/mL stearic acid-18, 18, 18-d_3 as the internal standard were added to 50 μL plasma samples for protein precipitation. The mixtures were vortexed for 10 min, sonicated for 10 min in an ice-water bath, and centrifuged for 10 min at 15,000 rpm. Then, 200 μL of the supernatant solution was evaporated to dryness using a ZLS-2 vacuum centrifugal concentrator. The dried residue was added to 80 μL of methanol/acetonitrile (50/50, v/v) for further metabolomic analysis. The quality control (QC) samples were prepared by mixing equal aliquots from each sample and processed following the above protocols.

Metabolite separation was achieved with an ACQUITY UPLC HSS T3 column (100 mm × 2.1 mm, 1.8 μm, Waters Corp., Milford, MA, USA). The mobile phase consisted of a mixture of ultrapure water (0.1% formic acid) and acetonitrile (0.1% formic acid). The elution program was as follows: 0–1.5 min, 0–5% B; 1.5–3.5 min, 5–35% B; 3.5–4.5 min, 35–50% B; 4.5–5.5 min, 50–70% B; 5.5–9.0 min, 70–100% B; 9.0–11.5 min, 100% B; 11.5–13.5 min, 100–0% B; 13.5–16.5 min, 0% B. The flow rate and oven temperature were 0.4 mL/min and 40 °C, respectively. The injection volumes of the samples were 1 μL and 3 μL for positive and negative ion modes, respectively. MS analyses were performed on a Waters Xevo-G2 XS Q-TOF MS system (Waters Corp., Milford, MA, USA). The MS parameters were set as follows: capillary voltage at 2.5 kV; cone voltage at 40 V and 35 V; and desolvation gas temperature at 400 °C and 450 °C for positive and negative modes, respectively. Source temperature at 110 °C; desolvation gas flow at 700 L/h; cone gas rate at 50 L/h; collision energy at 10–60 eV; scanning range of mass spectrometry at 50–1100 Da. All analyses were acquired using a LockSpray interface to ensure accuracy and reproducibility, and LE was used as the reference compound with m/z 556.2771 for ESI^+ and 554.2615 for ESI^-.

2.4. Metabolomic identification and data processing

UPLC-Q-TOF/MS raw data were processed by using Progenesis QI software (version 2.0, Waters, USA) for peak alignment, grouping, peak extraction, and peak identification operations. The raw data matrix was normalized by the QC samples and the intensity of internal standards. Then, SIMCA−P (v14.1; Umetrics, Umeå, Sweden) was performed on the normalized datasets for multivariate statistical analysis (MVA). The principal component analysis (PCA) model was applied to determine the clustering trend, and R^2 and Q^2 values were employed to evaluate the quality of PCA model. The combination of S plot of orthogonal partial least squares discriminant analysis (OPLS-DA) model and two-tailed Student's t-test or Mann Whitney U test [a false discovery rate (FDR)–adjusted P values < 0.05] was performed to identify the differentially expressed ion variables between HCC and LC groups. Metabolite identification for the differentiated ion-variables was performed by using the primary and secondary MS fragment information and the QI MetaScope, HMDB, METLIN, and LIPIDMAPS databases. The matched metabolite was further identified by the retention times and primary and secondary MS fragments of authentic standards using an in-house metabolite library.

2.5. Statistical analysis

For clinical variables, continuous and non-normally distributed variables are presented as the mean and standard deviation (means ± SD) and medians and interquartile ranges [IQRs] and were compared by two-tailed Student's t-test and Mann Whitney U test, respectively. Categorical variables were summarized by frequency (n) and percentages (%) and compared by using Chi-square test.

The correlation of metabolites with HCC was performed by univariate and multivariable regression analyses using SPSS Statistics 26 software (IBM Corp, New York, USA) and a bioinformatics platform (http://www.bioinformatics.com.cn/login/). FDR-calibrated $P < 0.05$ was considered significant. Relationships between clinical laboratory HCC-related markers (AFP, ALT, and AST) and metabolite signatures were calculated using a debiased sparse partial correlation (DSPC) network based on MetaboAnalyst software (http://www.metaboanalyst.ca/). Heatmap analyses of metabolic alterations were performed by using TBtools software v1.098769. Quantitative metabolic pathway analysis was performed by MetaboAnalyst using the Kyoto Encyclopedia of Genes and Genomes (KEGG) databases. The latent relationship network between biological functions and altered metabolites was generated based on the Ingenuity Pathway Analysis Database (IPA, QIAGEN Inc., German) and Cytoscape software v. 3.8.2. The random forest-based classification and feature ranking model were employed to select a small number of representative biomarkers that can maintain a maximized performance for differentiating HCC from LC in patients with HBV infection. The top metabolite biomarkers were selected based on the mean decrease in accuracy and receiver operating curve (ROC).

3. Results

3.1. Clinical characteristics of the study subjects

A total of 80 health individuals (male, 52.5%) and 332 patients with HBV infection participated in the study, including 224 LC patients with early HCC (male, 55.8%) and 108 LC patients without HCC (male, 53.7%). The clinical characteristics of all participants are summarized in Table 1. No differences in ages, gender, body mass index (BMI), smoking status, alcoholic consumption (>10 g/day), Child-Pugh class-calculated LC stages, and the prevalence of diabetes mellitus, hypertension, and coronary heart disease were observed between HCC and non-HCC groups. In clinical laboratory measures, there were no differences in the values of SBP, DBP, TC, TG, LDL-C, HDL-C, TBIL, DBIL, and blood glucose between HCC and non-HCC groups. However, the results indicated that patients with early HCC had higher values of AST, ALT, and AFP than patients without HCC.

3.2. Metabolic phenotypes of HBV-related LC patients with and without early HCC

The relative standard derivations (RSD) of the distribution for the detected ions in the QC samples are shown in Fig. 1A. The results showed that the ion variables with RSD <20% accounted for more than 85% of all detected variables in both the positive and negative models, indicating that the present metabolic analyses were stable. Then, an unsupervised PCA model was constructed to confirm the analytical reliability of the established metabolomic approach and capture the differences in the metabolic profiles of plasma samples from health controls and patients with and without early HCC. As shown in Fig. 2B, the QC samples were tightly clustered together in the PCA score plots of the datasets acquired in both the positive and negative models, suggesting the analytical reliability of the established metabolomic approaches. Furthermore, a clear clustering trend among health, HCC, and non-HCC groups was observed in the score plots, suggesting significantly different metabolic profiles between the study groups. The established PCA models were highlighted with powerful values of R^2 and Q^2, 0.621 and 0.843 for positive ion mode, 0.596 and 0.743 for negative ion mode, respectively.

3.3. Identification of early HCC-associated metabolite signatures

To characterize the differentiated metabolite signatures in patients with and without early HCC, *S*-plots of the orthogonal partial least squares discriminant analysis (OPLS-DA) model were constructed. As shown in Fig. 1C, a panel of ion variables was differentially expressed between patients with and without early HCC. Following the protocols of metabolite identification and verification (as described in the methods), a total of twenty-six differentiated metabolic alterations were identified, including seventeen chemical standard-annotated metabolites (Table 1). These altered metabolites mainly included bile acids, amino acids, lysophosphatidic acid (LysoPA), LysoPC, and PC. Although the PC species were not validated by chemical standards, they were confirmed by using other PC

Table 1
Demographic and clinical characteristics of the study subjects.

ID	Health controls (n = 80)	Early HCC patients (n = 224)	Non-HCC patients (n = 108)	P[a]
Male gender, n %	42, 52.50%	125, 55.80%	58, 53.70%	0.72
Ages	54.9 ± 9.86	56.1 ± 9.8	55.3 ± 10.9	0.5
Body mass index, kg/m^2	23.9 ± 1.9	24.6 ± 3.1	24.2 ± 3.6	0.42
Current smoker, n %	31, 38.75%	102, 45.54%	51, 47.22%	0.77
Alcoholic (>10 g/day), n %	23, 28.75%	89, 39.73%	41, 37.96%	0.76
Coronary heart disease, n %	5, 6.25%	12, 5.36%	7, 6.48%	0.68
Hypertension, n %	9, 11.25%	53, 23.66%	23, 21.30%	0.63
Mean office SBP, mmHg	124.1 ± 15.5	124.9 ± 17.2	123.6 ± 16.8	0.57
Mean office DBP, mmHg	80.1 ± 12.8	81.9 ± 10.5	81.3 ± 12.2	0.81
Diabetes mellitus, n %	7, 8.75%	21, 9.38%	13, 12.04%	0.45
Fasting blood glucose, mmol/L	5.43 ± 1.54	5.78 ± 1.83	5.65 ± 1.19	0.50
TG, mmol/L	0.98 ± 0.41	1.06 ± 0.57	1.16 ± 0.44	0.14
TC, mmol/L	3.96 ± 1.13	4.24 ± 0.57	4.34 ± 0.78	0.31
HDL-C, mmol/L	1.32 ± 0.24	1.19 ± 0.39	1.25 ± 0.29	0.18
LDL-C, mmol/L	2.59 ± 0.62	2.74 ± 0.76	2.79 ± 0.71	0.96
TBIL, μmol/L	13.83 ± 4.82	57.82 ± 20.84	59.72 ± 22.24	0.48
DBIL, μmol/L	2.48 ± 0.82	26.85 ± 10.95	28.51 ± 11.71	0.27
AST, mmol/L	22.42 [18.12, 27.65]	36.91 [25.47, 59.83]	23.51 [19.10, 31.09]	<0.0001
ALT, mmol/L	24.51 [17.46, 34.82]	40.81 [28.23, 67.34]	33.06 [23.68, 44.21]	0.0003
AFP, ng/mL	2.86 [1.46, 5.52]	16.09 [3.72, 180.12]	7.14 [6.47, 10.87]	0.0017
Child-Pugh class A, n %	/	198, 88.39%	95, 87.96%	0.91
Child-Pugh class B, n %	/	26, 11.61%	13, 12.04%	0.91

Continuous data are presented as mean ± standard deviation or median [interquartile range], categorical variables are presented as %. [a]: P value in the comparison of HCC and non-HCC. Two-tailed Student's *t*-test or Mann Whitney *U* test were used for continuous data. The Chi-square test was used for categorical data. HCC, hepatocellular carcinoma; SBP, systolic blood pressure; DBP, diastolic blood pressure; TG, triglycerides; TC, total cholesterol; HDL-C, high-density lipoprotein cholesterol; LDL-C, low-density lipoprotein cholesterol; TBIL, total bilirubin; DBIL, direct bilirubin; AST, aspartate aminotransferase; ALT, alanine aminotransferase; AFP, alpha-fetoprotein.

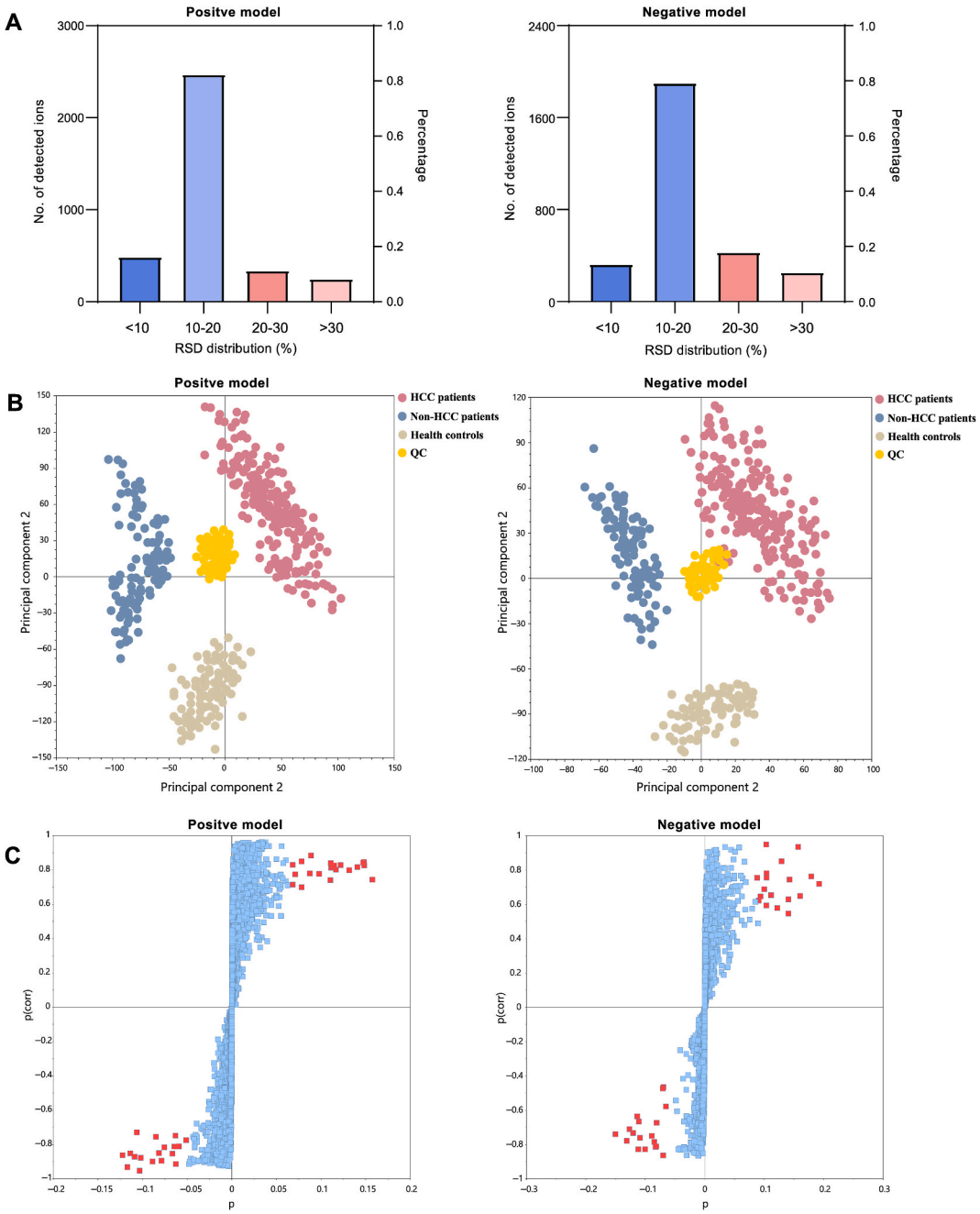

Fig. 1. Stability evaluation and multivariate statistical analysis of metabolomic data from health controls and patients with and without early HCC. (A) Stability of analytical methods based on the RSD distribution of detected ion variables in QC samples. **(B)** PCA score plots depicting the apparent assembly of QC samples and remarkable separation of the study groups. Each point represents an individual QC sample or real tested sample. **(C)** *S*-plot of OPLS-DA depicting profound metabolic alterations between patients with HCC and those without HCC. Upper right zone: metabolites that are more abundant in patients with HCC than in patients without HCC. Lower left zone: metabolites that are more abundant in patients without HCC than in patients with HCC.

standard chemicals and the specific fragment ion 184.1 in the positive MS model. The results of univariate statistical tests and fold changes of these altered metabolites between HCC and non-HCC groups are summarized in Table 2. Furthermore, we also calculated the expression trends of these differential metabolites in comparison of health controls with the HCC or non-HCC patients. As shown in Table S1, we found that all these plasma metabolite markers were differentially expressed between health controls and HCC patients. In contrast, only 21 metabolite biomarkers were statistically different between health controls and non-HCC patients. The overall heatmap of the altered metabolite markers revealed that the samples of patients with early HCC were clearly separated from the

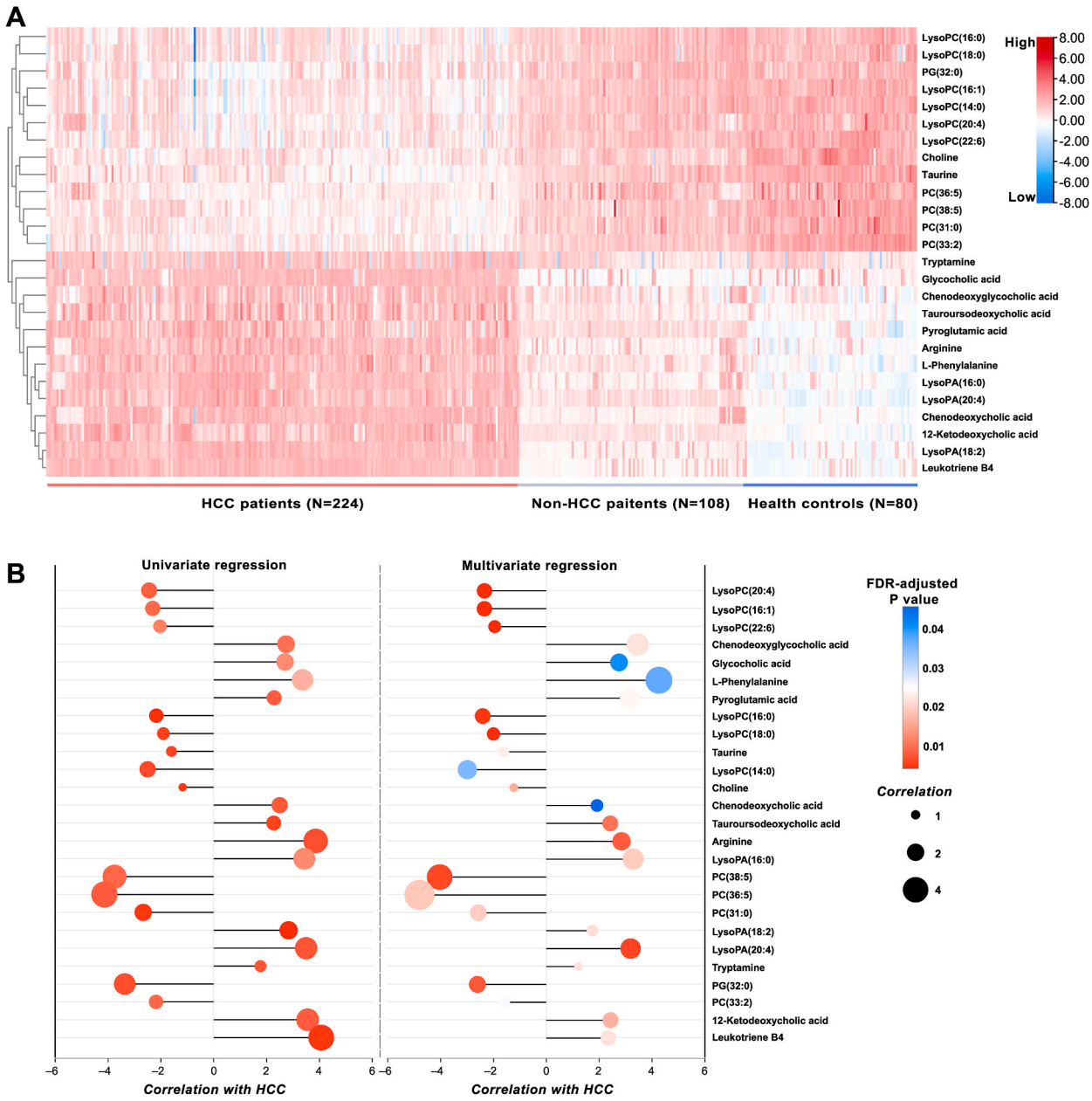

Fig. 2. Metabolite signatures and their association with early HCC. (A) Heat map of the differential metabolites that distinguish HCC from non-HCC patients and health controls. **(B)** Univariate and multivariate regression analysis plot depicting the association of each metabolite marker with HCC. Positive or negative correlation values indicate a positive or negative association of metabolites with HCC, and FDR-adjusted $P < 0.05$ was considered significant. In multivariate regression analysis, adjusted factors included ages, gender, body mass index, smoking/drinking status, Child-Pugh classes, diabetes mellitus, hypertension, coronary heart disease, and all clinical laboratory measures. The bubble size refers to the correlation intensity.

samples of non-HCC patients and health controls (Fig. 2A).

Then, we performed univariate and multivariate regression analyses to explore the associations of twenty-six metabolites with the condition of early HCC (Fig. 2B). Notably, the resultant plot indicated that all these metabolic markers were significantly correlated with HCC in the univariate model. Furthermore, the results indicated that all the metabolites remained significantly associated with HCC, even after adjusting for ages, sex, BMI, smoking/drinking status, Child-Pugh classes, AFP, AST, ALT, and other metabolic diseases, such as diabetes mellitus and hypertension. These results indicated that HBV-related LC patients with early HCC exhibited specific metabolite changes compared to those without HCC.

Table 2
Plasma metabolite markers for differentiating early HCC from non-HCC.

Metabolites	HMDB	log2(Fold changes)	P value	FDR-adjusted P value
Arginine[a]	HMDB0000517	1.50	4.95×10^{-30}	9.19×10^{-30}
Chenodeoxycholic acid[a]	HMDB0000518	1.60	4.06×10^{-27}	5.56×10^{-27}
Chenodeoxyglycocholic acid[a]	HMDB0006898	1.19	7.16×10^{-18}	7.16×10^{-18}
Choline[a]	HMDB0000097	−0.40	1.09×10^{-18}	1.13×10^{-18}
Glycocholic acid[a]	HMDB0000138	1.67	1.03×10^{-28}	1.67×10^{-28}
Leukotriene B4[a]	HMDB0001085	1.75	3.77×10^{-37}	9.80×10^{-36}
L-Phenylalanine[a]	HMDB0000159	0.62	4.75×10^{-31}	1.23×10^{-30}
LysoPA (16:0)[a]	HMDB0007853	2.06	7.36×10^{-32}	2.73×10^{-31}
LysoPA (18:2)	HMDB0007856	2.10	6.64×10^{-36}	8.63×10^{-35}
LysoPA (20:4)[a]	HMDB0114742	0.97	5.83×10^{-33}	3.03×10^{-32}
LysoPC(14:0)[a]	HMDB0010379	−1.35	8.20×10^{-35}	7.11×10^{-34}
LysoPC(16:0)[a]	HMDB0010382	−0.89	7.95×10^{-28}	1.22×10^{-27}
LysoPC(16:1)	HMDB0010383	−1.06	2.50×10^{-31}	7.21×10^{-31}
LysoPC(18:0)[a]	HMDB0010384	−0.86	2.88×10^{-24}	3.26×10^{-24}
LysoPC(20:4)[a]	HMDB0010395	−0.87	1.50×10^{-24}	1.77×10^{-24}
LysoPC(22:6)	HMDB0010404	−1.02	1.39×10^{-31}	4.51×10^{-31}
PC(31:0)	HMDB0007935	−0.67	5.75×10^{-33}	3.03×10^{-32}
PC(33:2)	HMDB0007940	−0.38	2.42×10^{-30}	4.84×10^{-30}
PC(36:5)	HMDB0007890	−1.28	2.23×10^{-27}	3.22×10^{-27}
PC(38:5)	HMDB0007989	−0.56	1.52×10^{-29}	2.64×10^{-29}
PG (32:0)	HMDB0010570	−1.39	1.28×10^{-26}	1.67×10^{-26}
Pyroglutamic acid[a]	HMDB0000267	0.58	4.86×10^{-26}	6.02×10^{-26}
Taurine[a]	HMDB0000251	−0.66	4.18×10^{-32}	1.81×10^{-31}
Tauroursodeoxycholic acid[a]	HMDB0000874	1.35	1.65×10^{-30}	3.58×10^{-30}
Tryptamine[a]	HMDB0000303	1.25	7.43×10^{-24}	8.05×10^{-24}
12-Ketodeoxycholic acid	HMDB0000328	0.87	1.54×10^{-30}	3.58×10^{-30}

Two-tailed Student's *t*-test or Mann Whitney *U* test was used for the comparison of HCC and non-HCC. A log2(fold change) value > 0 or <0 indicated that metabolites were increased or decreased in the plasma of patients with HCC compared to patients without HCC. [a] Chemical standard-annotated metabolites. FDR, false discovery rate; LysoPA, lysophosphatidic acid; LysoPC, lysophosphatidylcholine; PC, phosphatidylcholine; PG, phosphatidylglycerol.

3.4. Metabolic pathway and network analysis of early HCC-associated metabolites

To characterize the significant metabolic pathways and biological functions involved in the identified metabolite signatures that discriminated HCC and non-HCC patients, bioinformatics analysis was performed utilizing MetaboAnalyst and IPA software. As shown in Fig. 3A, four major KEGG pathways were enriched, including phenylalanine metabolism, glycerophospholipid metabolism, primary bile acid biosynthesis, and taurine and hypotaurine metabolism. To further understand the biological function of the differentiated metabolites, a functional relationship network was constructed using IPA knowledge database and Cytoscape. As depicted in Fig. 3B, the resultant network indicated that most of the metabolites were primarily involved in the metabolism of phospholipids and bile acids. Notably, the accumulation of L-phenylalanine, leukotriene B4, arginine, pyroglutamic acid, LysoPA species, and bile acid species and the reduction in taurine and PC species were significantly associated with the inflammatory response and oxidative stress. By using the major DSPC network analysis, we also investigated the potential associations of clinical and metabolic alterations in patients with early HCC. As shown in Fig. 3C, the inflammation-related metabolites, including LysoPA species and bile acid species, showed strongly positive interactions with each other. Furthermore, the results also demonstrated that bile acids, leukotriene B4, and a small pane of hydrophilic metabolites (such as arginine, phenylalanine, and pyroglutamic acid) showed significant correlations with APF, ALT, or AST.

3.5. Metabolite markers for identifying early HCC from patients with HBV-related LC

AFP is the most widely used tumor marker for HCC. Although our results indicated that the AFP levels of patients with early HCC were significantly higher than those of subjects without early HCC ($P = 0.0017$), the area under the receiver-operating curve (AUC-ROC) of AFP only yielded a very low value, 0.613 (as shown in Fig. 4A) for discriminating two study groups. To test whether the identified discriminatory metabolites could be used for identifying early HCC in the study population, we used a random forest-based machine learning feature selection method to select representative markers. The mean decreased importance values of twenty-six HCC-related metabolites are depicted in Fig. 4B. The ROC analyses of the top-ten metabolites are depicted in Fig. 4C. Notably, the AUC values of the top-ten metabolites ranged from 0.888 to 0.931. In addition, we found that most of these candidate markers were closely associated with inflammation responses (as shown in Fig. 3B). By using the random forest-based Monte-Carlo cross validation model, we identified the combination of the top-five metabolites (leukotriene B4, LysoPA 18:2, LysoPC 14:0, LysoPA 20:4, and glycocholic acid) as the best classifier (AUC-ROC = 0.981), while the additional features had little effect on the AUC values (Fig. 4D).

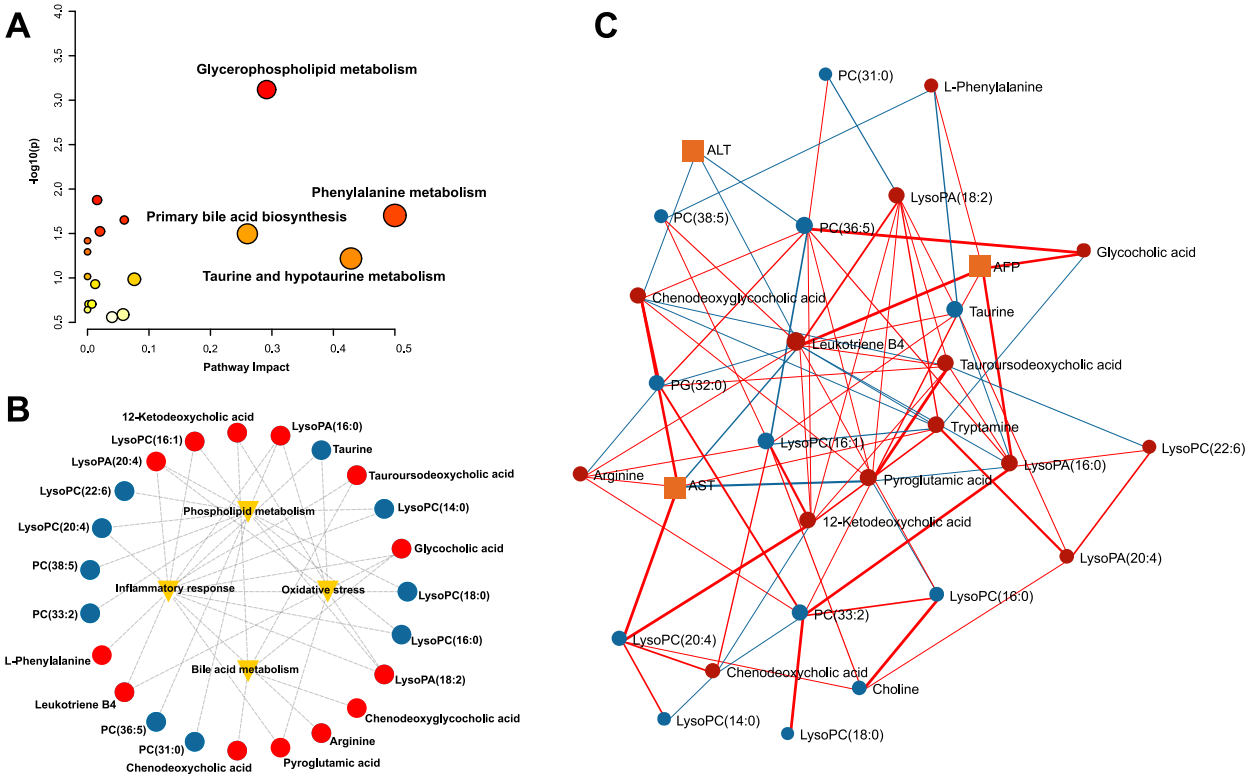

Fig. 3. Metabolism, function, and correlation network analyses of early HCC-related metabolite signatures. (A) Metabolic pathway analysis of the altered metabolites by using MetaboAnalyst. The color intensity and size of the circle are proportional to the enriched *P* value and pathway impact. Only pathways with $P < 0.05$ and impact >0.2 are labeled. **(B)** IPA database-based functional network of the metabolic signatures. The red and blue circles represent metabolites that were elevated and decreased in HCC compared to non-HCC, respectively. **(C)** Debiased sparse partial correlation network plot visualizing the major relationships of metabolic alterations and clinical markers; squares represent clinical variables, and the red and blue circles represent metabolites that were elevated and decreased in HCC in comparison to non-HCC, respectively. The red and blue solid lines indicate positive and negative correlations, respectively. The line intensity was proportional to the correlation values. (For interpretation of the references to color in this figure legend, the reader is referred to the Web version of this article.)

4. Discussion

In the current study, we demonstrated that HBV-related LC patients with early HCC exhibited remarkably differentiated plasma metabolome profiles compared to subjects without HCC. Through metabolic network and functional enrichment analyses, our study identified a variety of significant metabolites in multiple metabolic pathways that were implicated in inflammation responses and oxidative stress, providing an important link between metabolic dysfunction and HCC progression. Furthermore, regression and machine learning analyses identified a small panel of differentiated metabolites that exhibited powerful performances in the diagnosis of early HCC in high-risk patients with HBV-related LC.

Metabolites are not only substrates in metabolic activities but also signaling molecules controlling a wide range of cellular processes [29]. LysoPC is an important lysophospholipid subtype that derives from PC degradation. Its dysregulation has been associated with chronic HBV infection and tumorigenesis [30]. Our study indicated that several LysoPC species (such as 14:0, 16:0, 20:4, and 22:6) were remarkably decreased in patients with early HCC compared to those without HCC. Previous evidences have showed that LysoPC was significantly decreased in chronic liver diseases infected with HBV [31]. LysoPC was also considered a marker of malignant liver tumors and was significantly decreased in patients with HBV infection-related HCC [20,31]. Previous studies have demonstrated that LysoPC could play an important role in inhibiting tumor cell invasion and metastasis [32], and exhibited anti-inflammatory actions [31–33]. Thus, the decreased LysoPC levels suggested a higher anti-inflammation activation due to the existence of HCC in patients with HBV-related LC.

Another important finding of this study was that LysoPA species (including 18:2, 16:0, and 20:4) were significantly elevated in patients with early HCC. LysoPA refers to the downstream production of LysoPC [34]. Thus, the accumulation of LysoPA in patients with early HCC might be caused by largely decreased levels of LysoPC. LysoPA is a bioactive phospholipid that acts as a ligand for G protein-coupled receptors. Numerous studies have revealed that LysoPA could play critical roles in stimulating tumor cell proliferation and migration in various types of cancers, such as prostate cancer, breast cancer, ovarian cancer, and lung cancer [34–36]. Tumor-promoting inflammation is a key hallmark of LysoPA. LysoPA could promote the secretion of inflammatory mediators from

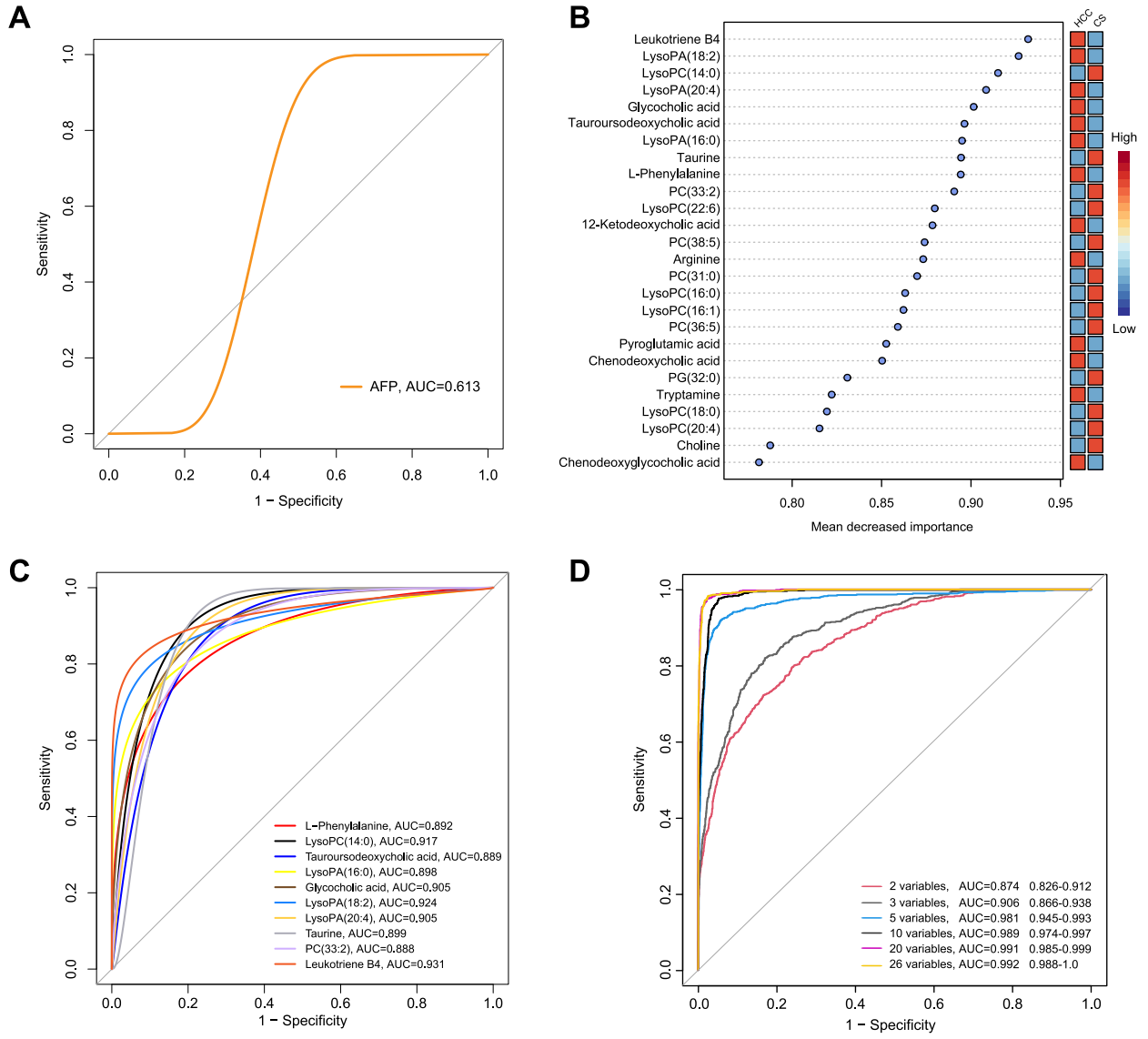

Fig. 4. Metabolite markers for diagnosing early HCC in HBV-related LC patients by using a random forest-based machine learning algorithm and receiver operating curve. **(A)** Logistic regression-based receiver operating curve (ROC) of the diagnostic performance for AFP. **(B)** Mean decreased importance-calculated plot of HCC-related metabolite markers. **(C)** Logistic regression-based ROC analyses of the diagnostic performances for the top ten metabolite markers. **(D)** Random forest-based receiver operating characteristic curve analyses of the diagnostic performances for multiple metabolite combinations.

tumor cells. The excess inflammatory mediators might also induce LysoPA production, which subsequently reinforces the inflammatory response, thus creating a vicious cycle that might be sustained [37–39]. Collectively, this evidence indicated that abnormal LysoPA signaling might be potential targets for ameliorating the development of HCC from HBV-related LC.

Compared to non-HCC subjects, we also found that five bile acids, including chenodeoxycholic acid, chenodeoxyglycocholic acid, glycocholic acid, tauroursodeoxycholic acid, and 12-ketodeoxycholic acid, together with arachidonic acid-derived leukotriene B4, were significantly increased in patients with early HCC. Emerging evidence has revealed that altered metabolite productions in bile acid metabolism were closely associated with HBV infection, chronic liver diseases, and liver carcinogenesis [40–42]. The elevated bile acids could directly activate protein kinase C, resulting in increased activation of nuclear factor kappa-B, ultimately leading to increased inflammation, oxidative stress, and cell proliferation [43]. Bile acids can also activate epidermal growth factor, leading to the upregulation of cyclooxygenase and lipoxygenase, which promote the production of reactive oxygen species and proinflammatory arachidonic acid derivatives [43,44].

Circulating biomarkers can facilitate the screening and early diagnosis of HCC with minimum invasion [20]. In clinical practice, the serum concentration of AFP is still the most widely used HCC biomarker so far, although numerous studies have demonstrated its

limited diagnostic sensitivity and specificity, especially in high-risk populations, including patients with LC and chronic HBV infection [45]. More recently, multi-marker combined detection has been considered a more powerful tool for the screening and early diagnosis of HCC [46,47]. By using regression and machine learning algorithms, this study identified a panel of five inflammation-related metabolites that might be used independently as biomarkers for detecting early HCC. Their combination yielded a significant discrimination performance in differentiating patients with early HCC from subjects without HCC (AUC-ROC of 0.981). These results suggested that the analyses of a small panel of metabolites might allow the specific and noninvasive diagnosis of early HCC in a high-cancerous risk population of patients with HBV-related LC.

Several limitations warrant discussion. The participants in the present study were Chinese people, which might limit the generalizability of our findings to other ethnic populations. Targeted metabolomics and larger cohort studies are needed to confirm our findings. Further studies investigating the mechanism of action of the key altered metabolites (such as LysoPA and bile acids) during HCC progression might be worthwhile.

5. Conclusions

In summary, this study identified a variety of bioactive metabolite alterations that showed high selectivity for detecting early HCC in patients with HBV-related LC, combining this with clinical insights might help clinicians ameliorate the screening and diagnostic practices of early HCC in high-risk patients suffering from HBV-related LC. Moreover, our findings provided important insights for the metabolic dysfunction and the early-stage HCC progression, allowing for the discovery of new therapeutic targets.

Author contribution statement

Pengfei Tu, Guoliang Zhang, Ying Ma, Yingyuan Lu: Conceived and designed the experiments, contributed reagents, materials, analysis tools or data. Zhiyong Du, Shengju Yin, Bing Liu, Wenxin Zhang, Jiaxu Sun, Meng Fang, Yisheng Xu, Kun Hua: Performed the experiments, analysed and interpreted the data. Zhiyong Du, Ying Ma, Yingyuan Lu: Wrote the paper.

Funding statement

This work was supported by the National Natural Science Foundation of China (Grant Nos. 82100295, 82104543, 82003904, 81773809), Key Laboratory of Natural and Biomimetic Drugs, Peking University (Grant No. K202227), Peking University Medicine Fund of Fostering Young Scholars' Scientific & Technological Innovation (Grant No. BMU2022PY013), and Scientific and Technological Innovation Project of China Academy of Chinese Medical Sciences (CI2021A04110). We acknowledge Waters Technologies Ltd. for their assistance in metabolomics analyses.

Data availability statement

Data will be made available on request.

Additional information

No additional information is available for this paper.

Declaration of competing interest

The authors declare that they have no known competing financial interests or personal relationships that could have appeared to influence the work reported in this paper.

Appendix A. Supplementary data

Supplementary data to this article can be found online at https://doi.org/10.1016/j.heliyon.2023.e16083.

References

[1] H.B. El-Serag, K.L. Rudolph, Hepatocellular carcinoma: epidemiology and molecular carcinogenesis, Gastroenterology 132 (7) (2007) 2557–2576.
[2] J.A. Marrero, L.M. Kulik, C.B. Sirlin, A.X. Zhu, R.S. Finn, M.M. Abecassis, et al., Diagnosis, staging, and management of hepatocellular carcinoma: 2018 practice guidance by the American association for the study of liver diseases, Hepatology 68 (2) (2018) 723–750.
[3] C. Peneau, S. Imbeaud, T. La Bella, T.Z. Hirsch, S. Caruso, J. Calderaro, et al., Hepatitis B virus integrations promote local and distant oncogenic driver alterations in hepatocellular carcinoma, Gut 71 (3) (2022) 616–626.
[4] C.J. Chen, H.I. Yang, J. Su, C.L. Jen, S.L. You, S.N. Lu, et al., Risk of hepatocellular carcinoma across a biological gradient of serum hepatitis B virus DNA level, JAMA 295 (1) (2006) 65–73.

[5] X. Gao, H.I. Yang, H. Trinh, D. Jeong, J. Li, J. Zhang, et al., Antiviral therapy and hepatocellular carcinoma risk in hepatitis B patients with cirrhosis, Eur. J. Gastroenterol. Hepatol. 32 (9) (2020) 1207–1211.
[6] D.H. Yang, W.P. Wang, Q. Zhang, H.Y. Pan, Y.C. Huang, J.J. Zhang, Hepatocellular carcinoma progression in hepatitis B virus-related cirrhosis patients receiving nucleoside (acid) analogs therapy: a retrospective cross-sectional study, World J. Gastroenterol. 27 (17) (2021) 2025–2038.
[7] Y. Lu, N. Li, L. Gao, Y.J. Xu, C. Huang, K. Yu, et al., Acetylcarnitine is a candidate diagnostic and prognostic biomarker of hepatocellular carcinoma, Cancer Res. 76 (10) (2016) 2912–2920.
[8] A. Quaglia, Hepatocellular carcinoma: a review of diagnostic challenges for the pathologist, J. Hepatocell. Carcinoma 5 (2018) 99–108.
[9] A. Singal, M.L. Volk, A. Waljee, R. Salgia, P. Higgins, M.A. Rogers, J.A. Marrero, Meta-analysis: surveillance with ultrasound for early-stage hepatocellular carcinoma in patients with cirrhosis, Aliment. Pharmacol. Ther. 30 (1) (2009) 37–47.
[10] Y. Guo, J. Zhao, J. Bi, Q. Wu, X. Wang, Q. Lai, Heterogeneous nuclear ribonucleoprotein K (hnRNP K) is a tissue biomarker for detection of early hepatocellular carcinoma in patients with cirrhosis, J. Hematol. Oncol. 5 (2012) 37.
[11] E.S. Jang, S.H. Jeong, J.W. Kim, Y.S. Choi, P. Leissner, C. Brechot, Diagnostic performance of alpha-fetoprotein, protein induced by vitamin K absence, osteopontin, dickkopf-1 and its combinations for hepatocellular carcinoma, PLoS One 11 (3) (2016), e0151069.
[12] H. Hanif, M.J. Ali, A.T. Susheela, I.W. Khan, M.A. Luna-Cuadros, M.M. Khan, D.T. Lau, Update on the applications and limitations of alpha-fetoprotein for hepatocellular carcinoma, World J. Gastroenterol. 28 (2) (2022) 216–229.
[13] S. Fang, L. Lai, J. Zhu, L. Zheng, Y. Xu, et al., A radiomics signature-based nomogram to predict the progression-free survival of patients with hepatocellular carcinoma after transcatheter arterial chemoembolization plus radiofrequency ablation, Front. Mol. Biosci. 8 (2021), 662366.
[14] S.M. Sanderson, J.W. Locasale, Revisiting the warburg effect: some tumors hold their breath, Cell Metabol. 28 (5) (2018) 669–670.
[15] C.T. Hensley, B. Faubert, Q. Yuan, N. Lev-Cohain, E. Jin, J. Kim, et al., Metabolic heterogeneity in human lung tumors, Cell 164 (4) (2016) 681–694.
[16] L. Chen, W. Lu, L. Wang, X. Xing, Z. Chen, X. Teng, et al., Metabolite discovery through global annotation of untargeted metabolomics data, Nat. Methods 18 (11) (2021) 1377–1385.
[17] L. Liang, F. Sun, H. Wang, Z. Hu, Metabolomics, metabolic flux analysis and cancer pharmacology, Pharmacol. Ther. 224 (2021), 107827.
[18] C. Pan, B. Li, M.C. Simon, Moonlighting functions of metabolic enzymes and metabolites in cancer, Mol. Cell. 81 (18) (2021) 3760–3774.
[19] X. Wang, A. Zhang, H. Sun, Power of metabolomics in diagnosis and biomarker discovery of hepatocellular carcinoma, Hepatology 57 (5) (2013) 2072–2077.
[20] P. Luo, P. Yin, R. Hua, Y. Tan, Z. Li, G. Qiu, et al., A Large-scale, multicenter serum metabolite biomarker identification study for the early detection of hepatocellular carcinoma, Hepatology 67 (2) (2018) 662–675.
[21] Y. Liu, Z. Hong, G. Tan, X. Dong, G. Yang, L. Zhao, et al., NMR and LC/MS-based global metabolomics to identify serum biomarkers differentiating hepatocellular carcinoma from liver cirrhosis, Int. J. Cancer 135 (3) (2014) 658–668.
[22] H. Cao, H. Huang, W. Xu, D. Chen, J. Yu, J. Li, L. Li, Fecal metabolome profiling of liver cirrhosis and hepatocellular carcinoma patients by ultra performance liquid chromatography-mass spectrometry, Anal. Chim. Acta 691 (1–2) (2011) 68–75.
[23] H.W. Ressom, J.F. Xiao, L. Tuli, R.S. Varghese, B. Zhou, T.H. Tsai, et al., Utilization of metabolomics to identify serum biomarkers for hepatocellular carcinoma in patients with liver cirrhosis, Anal. Chim. Acta 743 (2012) 90–100.
[24] D. Cui, W. Li, D. Jiang, J. Wu, J. Xie, Y. Wu, Advances in multi-omics applications in HBV-associated hepatocellular carcinoma, Front. Med. 8 (2021), 754709.
[25] M. Reig, A. Forner, J. Rimola, J. Ferrer-Fabrega, M. Burrel, A. Garcia-Criado, et al., BCLC strategy for prognosis prediction and treatment recommendation: the 2022 update, J. Hepatol. 76 (3) (2022) 681–693.
[26] Z. Du, Y. Du, L. Li, H. Sun, C. Hu, L. Jiang, et al., Metabolomic approach to screening homozygotes in Chinese patients with severe familial hypercholesterolemia, J. Clin. Med. 12 (2) (2023) 483.
[27] W. Dai, P. Yin, Z. Zeng, H. Kong, H. Tong, Z. Xu, et al., Nontargeted modification-specific metabolomics study based on liquid chromatography-high-resolution mass spectrometry, Anal. Chem. 86 (18) (2014) 9146–9153.
[28] T. Barri, L.O. Dragsted, UPLC-ESI-QTOF/MS and multivariate data analysis for blood plasma and serum metabolomics: effect of experimental artefacts and anticoagulant, Anal. Chim. Acta 768 (2013) 118–128.
[29] Y.P. Wang, J.T. Li, J. Qu, M. Yin, Q.Y. Lei, Metabolite sensing and signaling in cancer, J. Biol. Chem. 295 (33) (2020) 11938–11946.
[30] J. Yang, X. Zhao, X. Liu, C. Wang, P. Gao, J. Wang, et al., High performance liquid chromatography-mass spectrometry for metabonomics: potential biomarkers for acute deterioration of liver function in chronic hepatitis B, J. Proteome Res. 5 (3) (2006) 554–561.
[31] L. Zhou, L. Ding, P. Yin, X. Lu, X. Wang, J. Niu, et al., Serum metabolic profiling study of hepatocellular carcinoma infected with hepatitis B or hepatitis C virus by using liquid chromatography-mass spectrometry, J. Proteome Res. 11 (11) (2012) 5433–5442.
[32] P. Liu, W. Zhu, C. Chen, B. Yan, L. Zhu, X. Chen, C. Peng, The mechanisms of lysophosphatidylcholine in the development of diseases, Life Sci. 247 (2020), 117443.
[33] N.D. Hung, M.R. Kim, D.E. Sok, Anti-inflammatory action of arachidonoyl lysophosphatidylcholine or 15-hydroperoxy derivative in zymosan A-induced peritonitis, Prostag. Other Lipid Mediat. 90 (3–4) (2009) 105–111.
[34] P. Balijepalli, C.C. Sitton, K.E. Meier, Lysophosphatidic acid signaling in cancer cells: what makes LPA so special? Cells 10 (8) (2021) 2059.
[35] C.S. Chae, T.A. Sandoval, S.M. Hwang, E.S. Park, P. Giovanelli, D. Awasthi, et al., Tumor-derived lysophosphatidic acid blunts protective type I interferon responses in ovarian cancer, Cancer Discov. 12 (18) (2022) 1904–1921.
[36] Y.H. Lin, Y.C. Lin, C.C. Chen, Lysophosphatidic acid receptor antagonists and cancer: the current trends, clinical implications, and trials, Cells 10 (7) (2021) 1629.
[37] E. Kaffe, C. Magkrioti, V. Aidinis, Deregulated lysophosphatidic acid metabolism and signaling in liver cancer, Cancers 11 (11) (2019) 1626.
[38] F.M. Trovato, R. Zia, S. Napoli, K. Wolfer, X. Huang, P.E. Morgan, et al., Dysregulation of the lysophosphatidylcholine/autotaxin/lysophosphatidic acid axis in acute-on-chronic liver failure is associated with mortality and systemic inflammation by lysophosphatidic acid-dependent monocyte activation, Hepatology 74 (2) (2021) 907–925.
[39] S.A. Valdés-Rives, A. González-Arenas, Autotaxin-lysophosphatidic acid: from inflammation to cancer development, Mediat. Inflamm. 2017 (2017), 9173090, https://doi.org/10.1155/2017/9173090.
[40] X. Wang, G. Xie, A. Zhao, X. Zheng, F. Huang, Y. Wang, et al., Serum bile acids are associated with pathological progression of hepatitis B-induced cirrhosis, J. Proteome Res. 15 (4) (2016) 1126–1134.
[41] C.D. Fuchs, M. Trauner, Role of bile acids and their receptors in gastrointestinal and hepatic pathophysiology, Nat. Rev. Gastroenterol. Hepatol. 19 (7) (2022) 432–450.
[42] G. Xie, R. Jiang, X. Wang, P. Liu, A. Zhao, Y. Wu, et al., Conjugated secondary 12α-hydroxylated bile acids promote liver fibrogenesis, EBioMedicine 66 (2021), 103290, https://doi.org/10.1016/j.ebiom.2021.103290.
[43] W. Jia, G. Xie, W. Jia, Bile acid-microbiota crosstalk in gastrointestinal inflammation and carcinogenesis, Nat. Rev. Gastroenterol. Hepatol. 15 (4) (2018) 111–128.
[44] C.M. Payne, C. Bernstein, K. Dvorak, H. Bernstein, Hydrophobic bile acids, genomic instability, Darwinian selection, and colon carcinogenesis, Clin. Exp. Gastroenterol. 1 (2008) 19–47.
[45] M. Asrih, S. Lenglet, F. Mach, F. Montecucco, Alpha-fetoprotein: a controversial prognostic biomarker for small hepatocellular carcinoma, World J. Gastroenterol. 19 (3) (2013) 328–330.
[46] H. Yu, R. Han, J. Su, H. Chen, D. Li, Multi-marker diagnosis method for early Hepatocellular Carcinoma based on surface plasmon resonance, Clin. Chim. Acta 502 (2020) 9–14.
[47] H. Chen, Y. Zhang, S. Li, N. Li, Y. Chen, B. Zhang, et al., Direct comparison of five serum biomarkers in early diagnosis of hepatocellular carcinoma, Cancer Manag. Res. 10 (2018) 1947–1958.